IEEE Open Access Journal of
Power and Energy

Received 20 February 2024; revised 6 June 2024; accepted 10 July 2024.
Date of publication 16 July 2024; date of current version 31 July 2024.

Digital Object Identifier 10.1109/OAJPE.2024.3429390

A Holistic Approach to the Efficient Estimation of Operational Flexibility From Distributed Resources

NIKOLAOS SAVVOPOULOS[1] (Member, IEEE), NIKOS HATZIARGYRIOU[1,2] (Life Fellow, IEEE), AND HANNU LAAKSONEN[2] (Member, IEEE)

[1]School of Electrical and Computer Engineering, National Technical University of Athens, 157 72 Athens, Greece
[2]School of Technology and Innovations, University of Vaasa, 65200 Vaasa, Finland
CORRESPONDING AUTHOR: N. SAVVOPOULOS (nsavvopoulos@power.ntua.gr)

ABSTRACT The integration of Distributed Energy Resources (DER) like renewable generation into the power system has increased the need to develop effective strategies for procurement of flexibility services from these distribution network connected resources. In order to realize the flexibility potential of DERs to support flexibility needs of the system operators, the aggregated available flexibility at the interconnection point between transmission and distribution system needs to be estimated. This paper presents a novel optimization-based method to estimate the time-dependent flexibility at a primary distribution substation while accounting for the uncertainty of renewable generation. The proposed approach integrates the stochasticity of the flexibility resources using a scenario-based robust optimization and incorporates the intertemporal constraints of DER into the estimation process, ensuring a realistic representation of the flexibility capability over time. The scenarios are derived through sampling from a probability distribution of the renewable energy forecasts. This process utilizes a joint probability distribution and copulas to account for the temporal and spatial correlation among the renewable energy sources of the same region. Based on the joint hourly probability of the different scenarios a robust solution is finally obtained according to the assumed confidence level.

INDEX TERMS Active distribution grids, distributed energy resources, operational flexibility, optimal power flow (OPF), TSO-DSO coordination.

NOMENCLATURE

A. SETS AND INDICES

i	Index over distribution system nodes (buses).
l	Index over distribution system branches $l = (i, j)$ (lines).
ω	Index over scenarios.
g	Index over generation unit.
s	Index over batteries energy storage systems.
d	Index over loads.
$\mathbf{B}$	set of distribution system nodes (buses).
$\mathbf{L}$	set of distribution system branches (lines).
$\mathbf{T}$	set of time intervals.
Ω	set of selected scenarios.
$\mathbf{G}$	set of generation units of distribution system.
$\mathbf{G_i}$	set of generation units connected to bus i.
$\mathbf{FG}$	set of flexible generation units of distribution system (subset of $\mathbf{G}$).
$\mathbf{FG_i}$	set of flexible generation units connected to bus i.
$\mathbf{S}$	set of energy storage units.
$\mathbf{S_i}$	set of energy storage units connected to bus i.
$\mathbf{D}$	set of demand of distribution system.
$\mathbf{D_i}$	set of demand connected to bus i.
$\mathbf{FD}$	set of flexible demand of distribution system (subset of $\mathbf{D}$).
$\mathbf{FD_i}$	set of flexible demand connected to bus i.

B. OPTIMIZATION VARIABLES

$\delta p^G_{gt\omega}, \delta q^G_{gt\omega}$	Active/reactive power flexibility of generation unit g during time slot t and scenario ω.
$\delta p^S_{st\omega}, \delta q^S_{st\omega}$	Active/reactive power flexibility of storage unit s during time slot t and scenario ω.
$\delta p^D_{dt\omega}, \delta q^D_{dt\omega}$	Active/reactive power flexibility of demand d during time slot t and scenario ω.

$\delta p_{t\omega}^{TD}, \delta q_{t\omega}^{TD}$ Active/reactive power flexibility of distribution grid during time slot t and scenario ω.

$\delta p_{t}^{TD}, \delta q_{t}^{TD}$ Robust active/reactive power flexibility of distribution grid during time slot t.

$v_{it\omega}$ Voltage magnitude at bus i during time slot t and scenario ω.

$\theta_{it\omega}$ Voltage angle at bus i during time slot t and scenario ω.

C. PARAMETERS

P_{gt}^{G}, Q_{gt}^{G} Forecasted active/reactive power injected of generating unit g during time slot t.

P_{dt}^{D}, Q_{dt}^{D} Forecasted active/reactive power absorbed of demand d during time slot t.

P_{st}^{S}, Q_{st}^{S} Forecasted active/reactive power injected or absorbed of storage unit s during time slot t.

$\eta_{s}^{c}, \eta_{s}^{d}$ Charging/ discharging efficiency of battery energy storage system s.

$SoC_{st\omega}$ State-of-Charge of battery energy storage unit s during time slot t and scenario ω.

P_{t}^{TD}, Q_{t}^{TD} Active/reactive power injected or absorbed to distribution grid during time slot t.

$W_{gt\omega}^{P^G}, W_{gt\omega}^{Q^G}$ Active/reactive power deviation of generating unit g from its base case operating point during time slot t and scenario ω.

V_{i}^{min}, V_{i}^{max} Minimum and Maximum voltage limit of bus i.

$S_{l}^{F,max}$ Maximum flow limit of line l.

ϕ The angle of the selected search direction.

$P_{g}^{G_{min}}, P_{g}^{G_{max}}$ Minimum and Maximum active power generation limit for generation g.

$Q_{g}^{G_{min}}, Q_{g}^{G_{max}}$ Minimum and Maximum reactive power generation limit for generation g.

$\Delta P_{g}^{G+}, \Delta P_{g}^{G-}$ Upward/ downward active power flexibility limit offered by flexible generation g during time slot t.

$\Delta Q_{g}^{G+}, \Delta Q_{g}^{G-}$ Upward/ downward reactive power flexibility limit offered by flexible generation g during time slot t.

$PF_{g}^{lag}, PF_{g}^{lead}$ Lagging and leading power factor limit of the V-curve for generation g.

$\Delta P_{d}^{D+}, \Delta P_{d}^{D-}$ Upward/ downward active power flexibility limit offered by flexible demand d during time slot t.

$\Delta Q_{d}^{D+}, \Delta Q_{d}^{D-}$ Upward/ downward reactive power flexibility limit offered by flexible demand d during time slot t.

$\Delta P_{s}^{S+}, \Delta P_{s}^{S-}$ Upward/ downward flexibility limit offered by battery energy storage system s during time slot t.

S_{s}^{max} Maximum power capability limit of battery energy storage system s.

SoC_{s}^{-}, SoC_{s}^{+} Minimum/ maximum acceptable State-of-Charge level of battery energy storage system s.

I. INTRODUCTION

THE energy sector is undergoing a significant transformation, driven by the increasing need for clean and sustainable energy sources. The integration of an increasing amount of distributed Renewable Energy Sources (RES) in particular, leads to a paradigm shift in conventional power system operation. The traditional one-way power flow from the transmission system to the distribution system is evolving into a more complex bidirectional flow, highlighting the importance of the coordinated operation of the respective operators, Transmission System Operators (TSOs) and Distribution System Operators (DSOs) [1]. The interconnection point between transmission and distribution is the significant point through which energy flows from high to low voltage levels and vice versa.

The concept of flexibility in power systems has been formally introduced in [2], [3], and [4]. Flexibility was defined in [2] as ''the ability of a system to deploy its resources to respond to changes in net load''. In [3], flexibility is defined as ''the ability of a power system to cope with variability and uncertainty in both generation and demand, while maintaining a satisfactory level of reliability at a reasonable cost, over different time horizons''. Reference [4] reviews the concept of power system flexibility, and its role in ensuring power system security, while examines the origin, technical classification, and economic aspects of reserve.

In this paper, we specifically refer to the operational flexibility in terms of the feasible region of active (P) and reactive power (Q) adjustments at the TSO-DSO interconnection point. This operational flexibility is crucial for the controllability of P and Q flows, especially in the context of power systems with increasing penetration of Distributed Energy Resources (DERs) such as PVs, Battery Energy Storage Systems (BESS), and Electric Vehicles (EVs), at the distribution level.

A. PROBLEM DESCRIPTION

TSOs are responsible for managing the transmission system, while DSOs operate the distribution networks. In the near future, as the role of DSOs evolves, they are expected to also provide flexibility services to TSOs through the efficient coordination of local DERs [5]. This flexibility could be utilized to support the transmission network stable operation. A TSO-DSO flexibility curve is the area of active and reactive power capacity at the point of interconnection between TSO and DSO, which respects feasible operation of the distribution grid. The TSO-DSO flexibility curve depicts the aggregated available flexibility at the

interconnecting substation that the distribution system can offer to the transmission system [6].

The estimation of operational flexibility at the TSO-DSO interconnection point is a challenging task due to the time-dependent and stochastic nature of the power system operation. This difficulty arises from the inherent uncertainties associated with the generation of RES, the fluctuations in demand, and the operational constraints of DERs and network components.

Furthermore, traditional power system planning and operation methods, which often assume a static and deterministic system state, are inadequate to address the uncertain nature of modern power systems with a high share of renewables. As the uncertainty and variability of the operation of the power system is increasing, the need for efficient and reliable provision of flexibility services from DERs located in the distribution grid becomes increasingly important. A stochastic estimation of operational flexibility is thus necessary for a reliable proliferation of flexibility while ensuring the safe and efficient operation of both transmission and distribution system.

The purpose of this research paper is to propose a holistic approach for the efficient estimation of time-dependent operational active and reactive flexibility at the TSO-DSO interconnection point. The paper explores the integration of optimization models, and advanced statistical techniques to account for the uncertain aspects of renewable power generation. The proposed framework uses a scenario-based optimization to integrate the stochasticity of the flexibility resources and incorporates the inter-temporal constraints of distributed flexibility resources into the estimation process to ensure a realistic representation of the flexibility capability over time. The robustness of the flexibility curve is incorporated into the proposed framework by utilizing a probability density function considering the realizations of available flexibility under the scenarios. This approach enables the acquisition of a robust flexibility curve with a certain confidence level.

B. LITERATURE REVIEW

The methodologies to estimate the aggregated flexibility of DERs in the distribution grid at the interconnection point with the transmission system are typically classified into two main groups: (i) Monte-Carlo-based approaches [7], [8], [9] and (ii) optimization-based approaches [10], [11], [12], [13], [14], [15], [16], [17], [18], [19].

The optimization-based approaches, in contrast to Monte Carlo methods, aim to directly identify the boundaries of the flexibility area around an operating point. These methods focus on maximizing the active-reactive power flexibility that the distribution system can offer at the substation connecting TSO and DSO networks. Presented in the literature as more promising, these approaches require fewer calculation steps and directly identify the boundary of the flexibility area in a specified search direction at each step. A search direction is specified by the power factor, i.e., the ratio of the aggregated active over reactive powers. Reference [10] identifies the boundary conditions of the flexibility area by minimizing the reactive power import from the TSO for a selected set of active power setpoints. References [11] and [12] incorporate in the non-convex non-linear optimization-based approach the cost of flexibility and determine different curves depending on the associated cost. Reference [13] investigates the impacts of the grid components, such as tap changing transformers, active/reactive generation, and demand on the estimated flexibility. In both [11] and [13], first, the extreme points of the flexibility area are calculated, minimizing or maximizing the active and reactive power exchange between the TSO and DSO, followed by granulated calculations, based only on the active power exchange, so that the boundaries are refined. Reference [14] proposes to explicitly formulate the time-variant $P - Q$ capabilities of each type of flexibility-providing unit as constraint in the two-step optimization employed in [11] and [13]. References [15] and [16] neglect the time-dependency of the flexible DERs powers and focuses on the uncertainty of demand and stochastic generation, proposing robust approaches to determine the available flexibility. Reference [18] emphasizes on various aspects of DERs such as capacity, ramp, duration, and cost to determine different flexibility features. Reference [19] focuses on the real-time estimation of support provision capability in poorly observable distribution networks. The study enhances network state estimation accuracy but underscores the need to consider real-world constraints such as limited monitoring infrastructure.

References [20], [21], and [22] propose new modeling approaches to solve this problem. However, these studies tend to overlook critical constraints that are essential for practical implementation, such as real-time operational limits and dynamic grid conditions. Recently, the authors in [23] and [24] presented an interesting application of optimization-based approaches for aggregating the time-dependent flexibility that EVs can offer. However, both approaches neglect the network constraints, leading to a flexibility estimation that might not be feasible, resulting an overestimation of available flexibility.

Most of these works calculate the flexibility curve using deterministic predictions, neglecting important factors of the operational planning such as the inherent uncertainty in RES generation and the time-dependent restrictions of storage systems' operation. These limitations lead to inaccurate predictions of available flexibility in day-ahead or several-hour-ahead planning, required by power system operators (both TSOs and DSOs). Reference [25] provides a comprehensive review of methodologies for assessing feasible operating regions at the TSO–DSO interface. This paper discusses the challenges and future directions in TSO-DSO coordination, highlighting the need for more comprehensive constraint inclusion in modeling approaches. Our previous work focused on identifying the contribution of residential PVs and BESS (residential or utility scale) to the amount and

nature of the aggregated flexibility [26]. In this paper, we estimate the maximum available flexibility for each time-step and we explicitly take into account the contribution of each type of resources providing flexibility services (RES and BESS). This extends our previous work in [17] and [26] by integrating implicitly in the optimization problem the inter-temporal constraints of the flexibility resources and formulating a multi-period optimization problem, in order to represent the time-dependent flexibility. Moreover, the proposed methodology integrates in the optimization model the stochasticity of the flexibility resources with a scenario-based robust optimization. The scenarios are obtained through sampling from the probability distribution of the energy forecasts. The sampling is performed from a joint probability distribution using copulas in order to take into consideration the temporal correlation among the time series and spatial correlation among the RES of the same region. Within this framework, we propose two alternatives for deriving the robust flexibility curve: 1) Identifying the worst realization of the estimated flexibility under the scenarios to ensure robustness against the most unfavorable conditions; and 2) Applying Kernel Density Estimation (KDE) at each flexibility point to derive a probability density function, allowing for the extraction of robust flexibility with a specified level of confidence and offering a probabilistic approach to assess flexibility under varying conditions.

The contribution of this paper can be summarized as the introduction of a robust optimization framework that efficiently addresses the following aspects:

- **Modeling uncertainty in stochastic generation:** The proposed approach explicitly incorporates the uncertainty of stochastic generation into the optimization problem by using scenario-based modeling. This allows for a more realistic and practical representation of uncertainty.
- **Integration of time-dependent flexibility resources:** The proposed methodology integrates effectively the inter-temporal constraints of DERs, such as BESS, in the optimization problem. The methodology proposes the formulation of a multi-period optimization problem that schedules the time-dependent DERs to maximize the total daily summation of hourly flexibility.
- **Incorporating probabilistic forecasting using multivariate distributions:** The methodology efficiently integrates the probabilistic forecast in the optimization problem by generating scenarios using Gaussian copulas. This approach accounts for both temporal and spatial correlations, enhancing the accuracy and reliability of the forecasts.
- **Estimation of the flexibility curve under uncertainty:** The proposed methodology introduces a KDE-based method to derive the probability density function of available flexibility. This enables the efficient estimation of a robust flexibility curve with a chosen level of confidence.

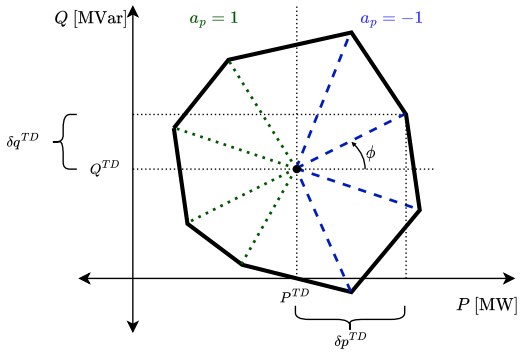

FIGURE 1. **Example of determining search directions for estimating flexibility at the TSO-DSO interconnection point.**

- **Holistic solution for TSO-DSO coordination:** By providing a holistic solution, the proposed framework improves the accuracy and reliability of flexibility estimation and enhances the coordination between TSOs and DSOs. This comprehensive approach ensures effective integration and operation of DERs within the power system.

II. ESTIMATING THE AGGREGATED FLEXIBILITY AT THE TSO-DSO INTERCONNECTION POINT

A. GENERAL OPTIMIZATION-BASED APPROACH

The optimization-based approaches estimate the flexibility curve taking into account the thermal limits of the distribution lines, the voltage constraints and the capability limits of the DERs to ensure no violation of the constraints in the distribution grid. The search direction of the method is determined by the power factor angle, as shown in Fig. 1. The general workflow of the method comprises three main steps:

1) Defining the search directions ϕ which outlines a search direction on the $P - Q$ plane. The angle can vary between 0° and 360° degrees and helps determine a_p and a_q that are used in the second step, for solving optimization problem as follows:

$$(a_p, a_q) = \begin{cases} (-1, 0), & 0^\circ \leq \phi < 90^\circ \\ (0, -1), & \phi = 90^\circ \\ (1, 0), & 90^\circ < \phi < 270^\circ \\ (0, 1), \phi = 270^\circ & \\ (-1, 0), & 270^\circ < \phi < 360^\circ \end{cases}$$

2) Computing the points of the flexibility curve by solving the optimization problem and identify one boundary feasible active-reactive power point of the flexibility curve.
3) Estimating the overall flexibility curve is performed upon defining the points of the flexibility curve. The overall flexibility curve is approximated by interpolating the boundary points.

B. INCORPORATING THE TIME-DEPENDENT DER FLEXIBILITY

The presence of time-dependent flexibility resources such as BESS, EVs, controllable loads, impacts the hourly total potential flexibility available at the TSO-DSO interface. These resources, especially BESS, have operational constraints that bound their current state of charge or discharge with the previous operational states. For instance, if a BESS is heavily discharged in one hour to support grid demand, its available flexibility to provide further support in the subsequent hours might be limited. Thus, the flexibility a BESS can offer is not just a function of its inherent capacity but also relies on its operational history and previous decisions.

Therefore, it is crucial to estimate the time-dependent flexibility as it takes into account the changing DER constraints, and hourly demand conditions across different periods. The results will be a set of flexibility areas that vary over time. The shape of the curves changes depending on the $P - Q$ capabilities of flexible resources and the state of the participating DER at each time step. A set of feasible and realistic flexibility maps for multiple time periods provides valuable input to the TSO for the daily operational planning. In this paper we use a multi-period optimization algorithm that aims to the maximization of the total available daily flexibility at the TSO-DSO interconnection point. The time-dependent flexibility estimation provides a more comprehensive and realistic view of the flexibility areas of distribution grids.

C. ESTIMATING THE FLEXIBILITY CURVE UNDER UNCERTAINTY

The proposed methodology estimates the robust flexibility curve using a scenario-based approach. The uncertainty of stochastic generation is explicitly modeled with scenarios which are used to derive a robust estimation of the available flexibility. The flowchart of the proposed method is presented in Fig. 2. The process begins by obtaining the probabilistic forecast for PV units production. This is used to create different scenarios for PV generation considering spatial-temporal correlations by a statistical method known as Copulas. To simplify calculations, deterministic forecast is considered for the demand, since the uncertainty of load forecast is generally much lower and the results of load forecasting more accurate. Moreover, the expected values of the probabilistic PV forecast are used to determine the schedule of BESS units, i.e. when they are used to locally optximize the exploitation of PV generation to meet the load demand, minimizing the energy exchange with the transmission system. The forecast and the BESS schedule are used to estimate the flexibility of the system for each hour over a 24-hour period for each set of PV generation scenarios. A polygon flexibility curve is then created using the flexibility points for each scenario. Finally, a robust solution is defined marking the worst-case scenario that aims to optimize the operation of the system under all possible scenarios.

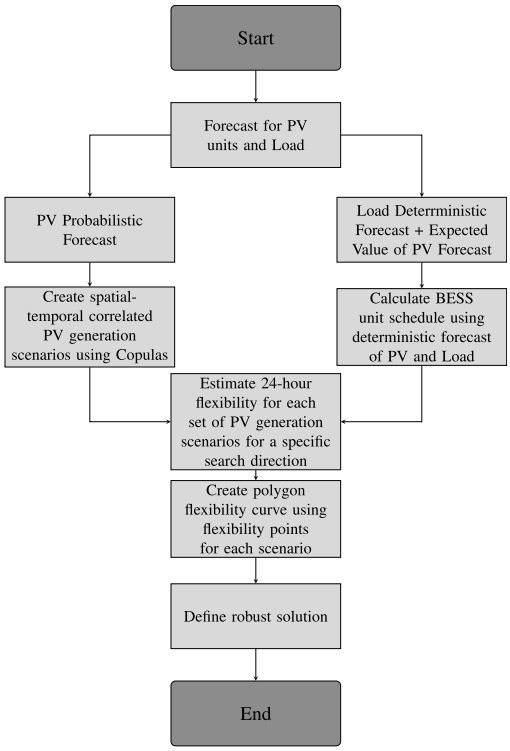

FIGURE 2. Flowchart of the proposed methodology.

III. PROBLEM FORMULATION

A. GENERAL MATHEMATICAL FORMULATION

This section describes the scenario-based robust optimization problem that determines the points of the time-dependent flexibility curve for a selected search direction.

Assuming $\phi \neq 90°, 270°$, the optimization problem is formulated as follows:

$$\min\ a_p \sum_{t}^{T} \delta p_t^{TD} + a_q \sum_{t}^{T} \delta q_t^{TD} \tag{1}$$

$$\text{subject to } \forall i \in \mathbf{B}, t \in \mathbf{T}, \omega \in \Omega$$

$$g(\psi) = 0 \tag{2a}$$

$$h(\psi) \leq 0 \tag{2b}$$

$$\delta p_{t\omega}^{TD} = \tan(\phi)\, \delta q_{t\omega}^{TD} \tag{2c}$$

$$\delta p_t^{TD} \leq \delta p_{t\omega}^{TD} \tag{2d}$$

$$\delta q_t^{TD} \leq \delta q_{t\omega}^{TD} \tag{2e}$$

where ψ denotes the set of optimization variables.

Therefore, the objective function (1) minimizes $-\delta p^{TD}$ (or equivalently maximizes δp^{TD}) when $a_p = -1$, which corresponds to positive values of δp^{TD} in quadrants 1 and 4. Similarly, the objective function minimizes δp^{TD} when $a_p = +1$, which corresponds to negative values of δp^{TD} in quadrants 2 and 3. Therefore at each point the objective function aims to maximize the flexibility provision at the TSO-DSO interface substation. Similarly, for search directions $\phi = 90°,\ 270°$, the objective function aims to maximize the reactive power flexibility δq^{TD} at the TSO-DSO interface and constraint (2c) is modified to set the active power flexibility

δp^{TD} to zero as follows:

$$\delta p^{TD} = 0 \tag{3}$$

B. TECHNICAL CONSTRAINTS OF DISTRIBUTION NETWORK

The net deviation of the active/ reactive power injection at node i from its base case operating point (for the selected time slot t) during the scenario ω can be written as:

$$\Delta P^{dev}_{it\omega} = \sum_{g}^{\mathbf{G_i}} W^{P^G}_{gt\omega} \tag{4a}$$

$$\Delta Q^{dev}_{it\omega} = \sum_{g}^{\mathbf{G_i}} W^{Q^G}_{gt\omega} \tag{4b}$$

Additionally, the net active/ reactive power injection flexibility that can be offered at node i for the selected time slot t during the scenario ω can be written as:

$$\Delta P^{flex}_{it\omega} = \sum_{g}^{\mathbf{FG_i}} \delta p^{G}_{gt\omega} + \sum_{s}^{\mathbf{S_i}} \delta p^{S}_{st\omega} - \sum_{d}^{\mathbf{FD_i}} \delta p^{D}_{dt\omega} \tag{5a}$$

$$\Delta Q^{flex}_{it\omega} = \sum_{g}^{\mathbf{FG_i}} \delta q^{G}_{gt\omega} + \sum_{s}^{\mathbf{S_i}} \delta q^{S}_{st\omega} - \sum_{d}^{\mathbf{FD_i}} \delta q^{D}_{dt\omega} \tag{5b}$$

The optimization is formulated using the non-linear AC power flow equations given by (6e), (6f). Constraints (6a)-(6d) enforce active and reactive power injection in each bus. 0 denotes the substation bus. Within the context of this paper, the proposed method is implemented using traditional optimization solvers for AC OPF, which have demonstrated considerable efficiency in managing the non-linear complexities of such optimization problems. However, considering the advancements in semidefinite programming and its growing application in this field, the proposed framework can be easily adapted and further increase the efficiency of the flexibility area estimation.

$$P_{it\omega} = \sum_{g}^{\mathbf{G_i}} P^{G}_{gt\omega} + \sum_{s}^{\mathbf{S_i}} P^{S}_{st\omega} - \sum_{d}^{\mathbf{D_i}} P^{D}_{dt\omega} + \Delta P^{flex}_{it\omega} + \Delta P^{dev}_{it\omega} \tag{6a}$$

$$P_{0t\omega} = \sum_{g}^{\mathbf{G_i}} P^{G}_{0t\omega} + \sum_{s}^{\mathbf{S_i}} P^{S}_{0t\omega} + P^{TD}_{0t\omega} - \sum_{d}^{\mathbf{D_i}} P^{D}_{0t\omega} + \Delta P^{flex}_{0t\omega} + \Delta P^{dev}_{0t\omega} \tag{6b}$$

$$Q_{it\omega} = \sum_{g}^{\mathbf{G_i}} Q^{G}_{gt\omega} + \sum_{s}^{\mathbf{S_i}} Q^{S}_{st\omega} - \sum_{d}^{\mathbf{D_i}} Q^{D}_{dt\omega} + \Delta Q^{flex}_{it\omega} + \Delta Q^{dev}_{it\omega} \tag{6c}$$

$$Q_{0t\omega} = \sum_{g}^{\mathbf{G_i}} Q^{G}_{0t\omega} + \sum_{s}^{\mathbf{S_i}} Q^{S}_{0t\omega} + Q^{TD}_{0t\omega} - \sum_{d}^{\mathbf{D_i}} Q^{D}_{0t\omega} + \Delta Q^{flex}_{0t\omega} + \Delta Q^{dev}_{0t\omega} \tag{6d}$$

$$P_{it\omega} = v_{it\omega} \sum_{k=1}^{N} [v_{kt\omega}(G_{ik}\cos(\theta_{it\omega} - \theta_{kt\omega}) + B_{nk}\sin(\theta_{it\omega} - \theta_{kt\omega})] \tag{6e}$$

$$Q_{it\omega} = v_{it\omega} \sum_{k=1}^{N} [v_{kt\omega}(G_{ik}\sin(\theta_{it\omega} - \theta_{kt\omega}) - B_{nk}\cos(\theta_{it\omega} - \theta_{kt\omega})] \tag{6f}$$

$$V_i^{min} \le v_{it\omega} \le V_i^{max} \tag{7a}$$

$$0 \le S_l \le S_l^{F,max} \quad \forall\, l \in \mathbf{L} \tag{7b}$$

C. MODELING THE CAPABILITY LIMITS OF DERS

The capability curves describe the limits of the active and reactive power that a generator can provide. These curves establish a boundary that covers all feasible operating points on the MW/MVAr plane. The power capability curves are typically nonlinear but within the context of this paper a linearized approximation is adopted. Following in this section the modeling and the operational flexibility capability are further presented and analyzed.

1) DISTRIBUTED GENERATION

DERs are capable of providing downward reserve and voltage support thanks to the flexibility of the converters, their $P-Q$ capability curves are usually assumed to be in the form of a "V-Curve" and are dependent on the power production and therefore are time-variant [14], [17]. The generators may also have different shapes of capability curves such as rectangular and D-shapes. The rectangular and D-shapes of the curve theoretically allow using the generator to provide voltage regulation services even when the unit does not produce active power (due to low wind or no sun), essentially working as a static synchronous compensator. The additional constraints for modeling the flexibility provision of distributed generation are:

$$P_g^{G_{min}} \le P^G_{gt} + W^{P^G}_{gt\omega} + \delta p^G_{gt\omega} \le P_g^{G_{max}} \tag{8a}$$

$$Q_g^{G_{min}} \le Q^G_{gt} + W^{Q^G}_{gt\omega} + \delta q^G_{gt\omega} \le Q_g^{G_{max}} \tag{8b}$$

$$\Delta P_g^{G_-} \le \delta p^G_{gt\omega} \le \Delta P_g^{G_+} \tag{8c}$$

$$\Delta Q_g^{G_-} \le \delta q^G_{gt\omega} \le \Delta Q_g^{G_+} \tag{8d}$$

$$-\arccos PF_g^{lag} \le \arctan \frac{P^G_{gt} + W^{P^G}_{gt\omega} + \delta p^G_{gt\omega}}{Q^G_{gt} + W^{Q^G}_{gt\omega} + \delta q^G_{gt\omega}} \tag{8e}$$

$$\arctan \frac{P^G_{gt} + W^{P^G}_{gt\omega} + \delta p^G_{gt\omega}}{Q^G_{gt} + W^{Q^G}_{gt\omega} + \delta q^G_{gt\omega}} \le \arccos PF_g^{lead} \tag{8f}$$

2) DEMAND-SIDE FLEXIBILITY

Flexibility from the demand side can be achieved by allowing the system operator to control, or provide price signals to,

various electricity demand devices, including power-to-heat, power-to-hydrogen, electric vehicle chargers, smart appliances, and industrial demand components. In this paper, continuous flexibility domain for these resources is considered. The capability curve has simple rectangular boundaries and represents loads with variable reactive power. The additional constraints for modeling the flexibility provision of controllable loads are:

$$\Delta P_d^{D-} \leq P_{dt}^D + \delta p_{dt\omega}^D \leq \Delta P_d^{D+} \tag{9a}$$

$$\Delta Q_d^{D-} \leq Q_{dt}^D + \delta q_{dt\omega}^D \leq \Delta Q_d^{D+} \tag{9b}$$

3) DISTRIBUTED BATTERY ENERGY STORAGE SYSTEMS

BESS have the ability to absorb and inject active power. Thanks to their interface via power electronic converters, they also have the potential to provide reactive power. The capability chart is often described as a circle, defined by the current limitations of the power converter. In our approach we have adopted a linearized rectangular approximation of the BESS capability curve, equipped with four-quadrant capability. The additional constraints for modeling the flexibility provision of BESS are:

$$\Delta P_s^{S-} \leq \delta p_{st\omega}^S \leq \Delta P_s^{S+} \tag{10a}$$

$$\Delta Q_s^{S-} \leq \delta q_{st\omega}^S \leq \Delta Q_s^{S+} \tag{10b}$$

$$(P_{st}^S + \delta p_{st\omega}^S)^2 + (Q_{st}^S + \delta q_{st\omega}^S)^2 \leq (S_s^{max})^2 \tag{10c}$$

$$SoC_{st\omega} = \sum_{\tau=1}^{t} (P_{s\tau}^S + \delta p_{s\tau\omega}^S) \tag{10d}$$

$$SoC_s^- \leq SoC_{st\omega} \leq SoC_s^+ \tag{10e}$$

IV. ILLUSTRATIVE EXAMPLE

A. DISTRIBUTION SYSTEM

We estimate the flexibility that can be provided by PVs, BESS and controllable loads at the TSO-DSO interface, using a 33-bus radial distribution system, as shown in Fig. 3. The distribution system contains 4 PV+BESS systems in buses 8, 22, 24 and 30, 3 PV systems in buses 4, 17 and 32 and 4 controllable loads in buses 7, 14, 25, 31. The implementation is performed in MATLAB using YALMIP as the modeling layer [27] and IPOPT as the solver [28].

We demonstrate the proposed methodology for a scheduling horizon of one day with hourly resolution. Fig. 4 presents the probabilistic PV generation forecast and the BESS charging/discharging schedule for a PV system located at bus 32 and for a PV+BESS system located at bus 24. Each BESS is assumed to be locally controlled to reduce the net demand of the specific bus. Therefore, the base case schedule of each BESS is determined using the deterministic forecast of the corresponding PV system in order to maximize the self-consumption by charging during the morning hours when there is excess PV energy and discharging later in the day when the demand is higher and PV generation reduces gradually to zero.

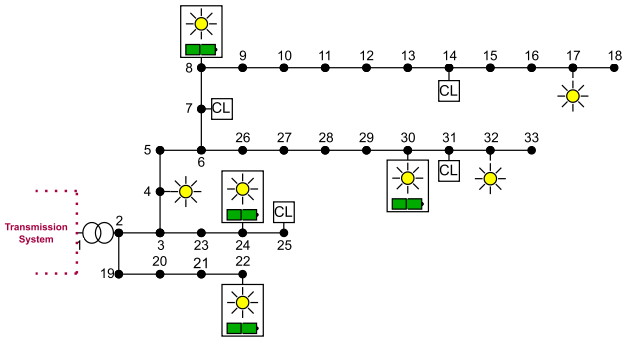

FIGURE 3. 33 bus distribution system.

B. MODELING RES UNCERTAINTY

The uncertainty associated with PV generation is integrated by employing the scenario approximation technique. This approximation approach allows the representation of complex, high-dimensional uncertainties with a set of scenarios in the non-linear, non-convex optimization problem, simplifying the computational burden while maintaining accuracy of the solution. The ability to adjust the number of scenarios allows an optimal balance between computational effort and the precision of the solution.

Probabilistic models, used in energy generation forecasting and scenario generation methods, are usually parametric models, that estimate the parameters of marginal probability distributions, for each unit and time step. These marginal distributions are considered independent and do not capture the spatio-temporal dependencies between the different time steps and the different units, although a RES unit generation is correlated with the neighboring units of the same technology. The effectiveness of the proposed framework under uncertainty is highly dependent on the quality of the forecast. Accurate forecasts of RES generation are crucial for reliable flexibility assessments. As part of this study, we use forecasts developed by the forecasting method presented in [29], which ensures high accuracy and robustness.

Generating scenarios using a typical sampling method has several limitations since it neglects these temporal and spatial correlation. Thus, realistic distributions should consider the auto-correlation of the RES generation time series and their spatial correlation. The use of copulas for the generation of multivariate distributions resolves these issues and enables the sampling accounting for the spatial and temporal correlation of RES forecast [30]. Copulas are mathematical constructs used to model and study the dependence structure between random variables. A copula enables the separation of the marginal distributions from the dependence structure.

In the presented test case, the sampling method is based on Gaussian copulas and marginal distributions for each RES unit produced by the parametric probabilistic forecasting model [29]. The method for generating the scenarios is performed as follows:

1) Generate samples from the constructed Gaussian copula $\mathbf{z}_{\mathbf{t},\mathbf{g},\omega} \sim c_Z(\boldsymbol{\mu}, \boldsymbol{\Sigma})$
2) Compute the inverse cumulative distribution function (ICDF) for each marginal distribution of the copula $\mathbf{P}^{\mathbf{G}}_{\mathbf{t},\mathbf{g},\omega} = F^{-1}_{t,g}(\mathbf{u}_{\mathbf{t},\mathbf{g},\omega})$
3) Transform the uniform samples $\mathbf{u}_{\mathbf{t},\mathbf{g},\omega}$ to the original domains $\mathbf{P}^{\mathbf{G}}_{\mathbf{t},\mathbf{g},\omega} = F^{-1}_{t,g}(\mathbf{u}_{\mathbf{t},\mathbf{g},\omega})$ for the t^{th} time step and g^{th} unit.

Fig. 5 graphically compares a set of 10 sampling scenarios of sampling for a PV unit using a standard sampling approach and the proposed sampling approach from multivariate distributions. Fig. 5(b) illustrates that the generated scenarios present both temporal and spatial correlations. For example, incorporating temporal correlations indicates that the scenarios do not develop as random time series throughout the examined day with increased abnormal shifts from one instance to the next as in Fig. 5(a). Spatial correlations indicate that variations in one PV unit often mirror or influence the behavior of other PV units in the same region.

The significance of time and space in PV generation is illustrated through the covariance matrix as depicted in Fig. 6. The matrix is segmented into submatrices, each representing the covariance of PV generation over time between pairs of PV parks. For instance, a specific section of the matrix, as highlighted in the zoomed-in area, details the covariance relationship between PV 1 and PV 2. The diagonal elements of the matrix represent the self-covariance of PV generation at individual time steps. Notably, as the time lag increases, there is a decrease in the absolute values of covariance, indicating a reduction in time-dependency. Furthermore, the off-diagonal elements, which represent the covariance between different time steps, reveal a spatial dependency. More specifically, for adjacent time steps a significant spatial dependency is identified, driven by similar weather conditions that affect PVs at adjacent geographical locations. Details for the creation of the joint distributions using Copulas are provided in Appendix.

Typically the robust flexibility curve is derived by identifying the worst realization of the estimated flexibility under the scenarios, as demonstrated in [15]. In addition to these approaches, this paper proposes a KDE-based approach that can extract a robust flexibility with a specified level. The generation of adequate number of scenarios at each time step can be used to obtain the probability density function of the available flexibility at this time step by applying a KDE method. This allows the extraction of flexibility values with specified confidence levels. It should be noted that the use of probability density functions provides a smoothed representation of the flexibility values, highlighting the general trend without getting overshadowed by individual extreme scenarios. The proposed approach offers a more holistic view of grid's flexibility under varying conditions of RES generation.

V. SIMULATION RESULTS

The performance of the proposed methodology in estimating the flexibility curve is explored through two distinct

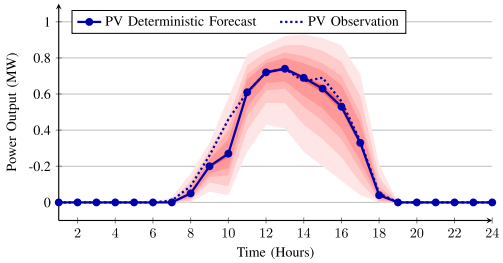

(a) PV System at bus 32

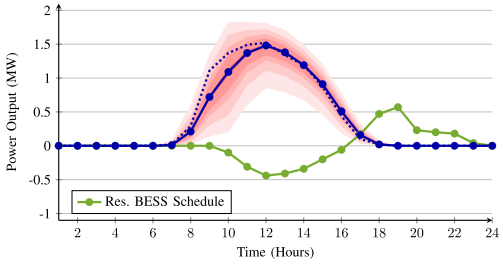

(b) PV+BESS System at bus 24

FIGURE 4. Forecast for PV production and BESS charging/discharging of the distribution network for a day with high solar PV generation.

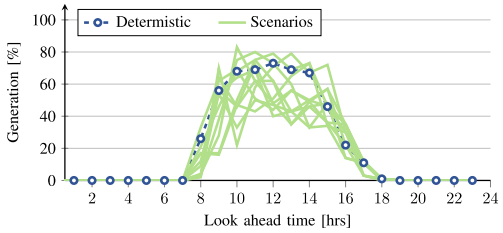

(a) Time Independent Scenarios

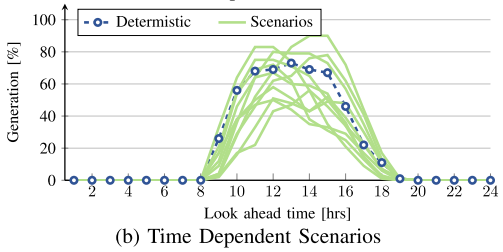

(b) Time Dependent Scenarios

FIGURE 5. PV generation scenarios using a standard sampling approach (a) and sampling from a joint probability distribution (b).

test cases: one without considering the inter-temporal constraints of the DERs (Subsection-A), and the other with these constraints (Subsection-B). In Subsection-A and -B, the stochastic flexibility curves presented depict both the expected and the robust flexibility curves. The expected curve is derived through a deterministic optimization process using the deterministic estimations of the PV generation, and the robust curve is represented by the worst realization of the estimated flexibility. Subsequently, in Subsection-C, the proposed KDE-method is applied to the scenarios already estimated in the previous subsections to derive the flexibility curve with a specified confidence level, providing

a probabilistic approach to assessing flexibility under uncertainty.

A. ESTIMATION OF AGGREGATED FLEXIBILITY WITHOUT CONSIDERING THE INTER-TEMPORAL CONSTRAINTS

This approach leads to an overestimated and unrealistic flexibility curve. This limitation is driven by the assumption that the flexibility provided by DERs is fully available at each hour. Even if the DSO had full control of the PV units and it is assumed that their expected generation is fully available, it cannot be applied to BESS and controllable loads, since the available flexibility strongly relies on the status of the previous/next hours. Fig. 7 presents the results for 4 different hours during the day namely:

- when PV units are not producing and the batteries are fully discharged (at hour 7),
- when PV units are producing and the BESS charge and store the excess energy (at hour 12), when PV units are producing but not enough to cover the local demand and the BESS are discharging to provide the stored energy (at hour 19) and
- when PV units are not producing but batteries contribute and cover part of the demand (at hour 22).

Each figure (Fig 7(a)-(d)) depicts the flexibility curve calculated with the expected PV generation (dashed curve), the flexibility curves for the scenarios (light green curves), and the robust flexibility curve of the scenario approximation method (dark green curve). The robust flexibility curve is obtained by the worst realization of the flexibility curve for the scenarios at each specified search direction. Estimated flexibility is represented from the viewpoint of the TSO, i.e. positive values for active/reactive power flexibility signify an increase in net demand within the distribution network, leading to the TSO supplying more energy to the DSO. Similarly, negative values indicate a decrease in net demand, resulting in the DSO providing more energy to the TSO.

During the first hours of the day (Fig. 7 (a)), PV units do not generate and BESS units do not have any stored energy, so only downward flexibility can be offered by charging BESS. Following during the day (Fig. 7 (b)), when PV units generate more than the local demand, and BESS store the excess energy, the distribution system can offer both upward and downward flexibility. The downward flexibility can be offered either by the PV generation or by the BESS increasing charging since they are not fully charged. Upward flexibility can be offered by providing the stored energy. When local demand is lower than solar power generation as in hour 19 (Fig. 7 (c)), BESS starts charging to cover additional energy demand. During these hours the distribution system can again offer both upward and downward flexibility by reducing the PV generation and controlling the BESS discharging. During the last hours of the day (Fig. 7 (d)), PV units do not generate again and BESS units can offer the remaining stored energy as upward flexibility or increase the discharge for downward flexibility.

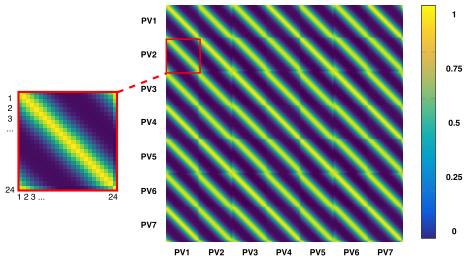

FIGURE 6. **Visualization of correlation matrix for the PV generation forecast.**

B. ESTIMATION OF AGGREGATED FLEXIBILITY CONSIDERING THE INTER-TEMPORAL CONSTRAINTS

In the second test case, the same scenarios are used. Integrating in the optimization problem the inter-temporal constraints for the flexibility provision of BESS provides a more realistic flexibility curve since it internally optimizes each BESS unit's operation schedule aiming to maximize the total available flexibility over 24 hours.

Fig. 8 presents the results for the same hours as in the previous section for the flexibility curves. The optimization problem internally determines the optimal scheduling of the time-dependent flexibility resources to maximize the amount flexibility that can be provided from the whole distribution system in the examined day. By comparing the curves displayed in Fig. 7 and Fig. 8, we observe a significant reduction of available flexibility provision, especially during the hours that PV generation is expected to be high. The introduction of inter-temporal constraints in the optimization problem reduces the available flexibility in some hours of the day providing feasible and more realistic results.

Fig. 9 addresses the computational efficiency aspect of the optimization framework by presenting the execution times required to calculate the flexibility curves for the two test cases with varying numbers of scenarios. The results show that the execution time increases significantly as the number of scenarios grows, particularly when temporal constraints are included. To tackle this issue, integrating parallel processing techniques into the optimization framework can substantially enhance computational efficiency. By leveraging parallel processing, it becomes feasible to handle a bigger distribution system with a large number of scenarios, even with temporal constraints, within reasonable time frames. This ensures the applicability of the proposed framework for its integration to TSO-DSO coordination schemes for the provision of flexibility services from DERs.

C. EVALUATION OF ROBUST FLEXIBILITY CURVE UNDER UNCERTAINTY

To better demonstrate the impact of the uncertainty of RES on the robust flexibility curve, the proposed KDE-based approach is applied to the estimated flexibility points. Fig. 10

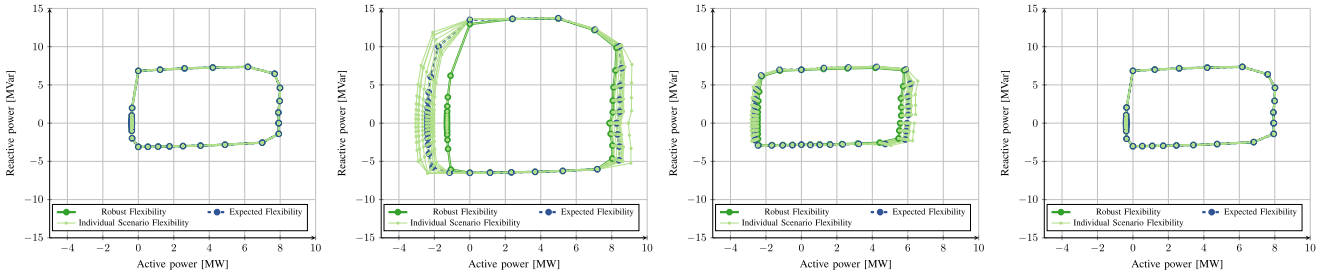

(a) Hour 7 (b) Hour 12 (c) Hour 19 (d) Hour 22

FIGURE 7. Estimated available flexibility area (without the inter temporal constrains) at 4 different hours of the day.

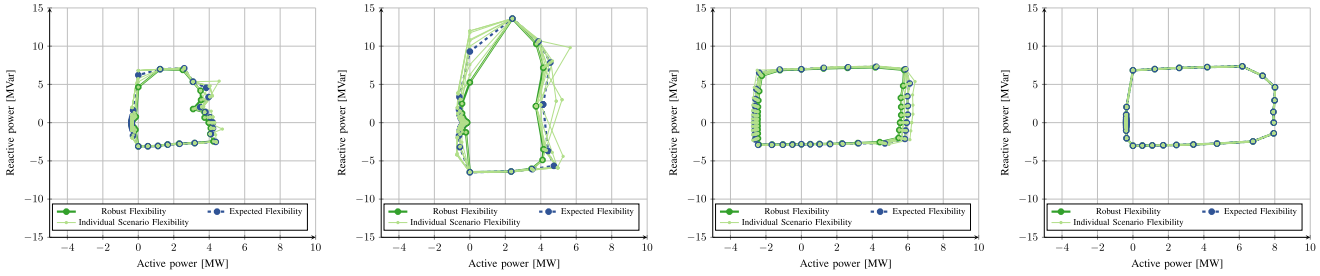

(a) Hour 7 (b) Hour 12 (c) Hour 19 (d) Hour 22

FIGURE 8. Estimated actual flexibility area (considering the inter temporal constraints) at 4 different hours of the day.

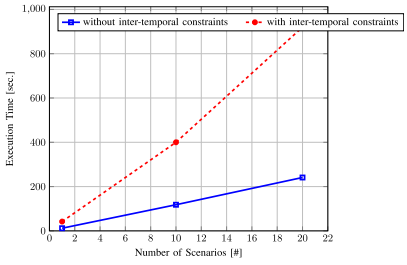

FIGURE 9. Comparison of execution time.

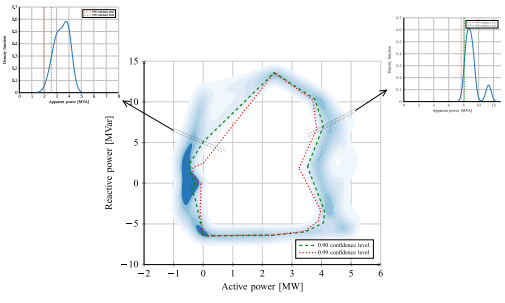

FIGURE 10. Uncertainty map and robust flexibility curve for different confidence levels at Hour 12 (Fig. 8 (b)).

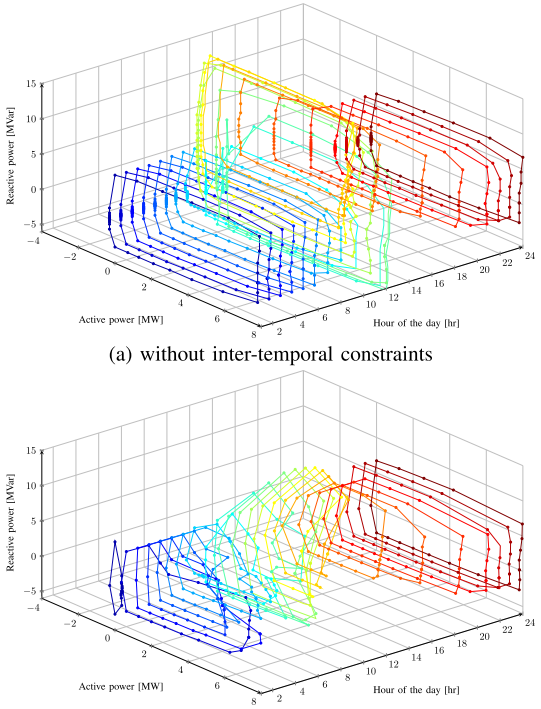

(a) without inter-temporal constraints

(b) with inter-temporal constraints

FIGURE 11. Multi-period robust flexibility area with 0.99 confidence level.

presents the uncertainty map and the robust flexibility curves of the distribution grid at Hour 12 (considering also the inter-temporal constraints) under the varying scenarios of RES generation. Two distinct curves are plotted, representing two confidence levels: 99% (red dotted) and 90% (green dashed). These curves depict the robust flexibility of the grid, ensuring that the grid can achieve the indicated flexibility with the respective confidence level. The resulting flexibility map aims at capturing the intricacies of different search directions.

Additionally, Fig. 10 presents the estimated distribution for apparent power flexibility provision that was obtained for various search directions. The distribution is unique at each search direction since it is created by the kernels that were added at the specific search direction. The results indicate that as the confidence level increases, the size of the flexibility map decreases. This is expected, as a higher confidence level implies a more conservative estimate, ensuring that the grid can handle the indicated flexibility under more tight conditions. However, in areas where the provision of reactive power is high, the robust flexibility curves converge and become identical. This is attributed to the fact that DERs can offer similar amounts of reactive power without violating the voltage limits under varying conditions of RES generation. As a result, despite varying conditions, the grid exhibits similar flexibility characteristics in regions where reactive power is dominant.

Fig. 11 present the hourly results of the estimated robust flexibility curves with 0.99 confidence level over a 24-hour period. The multi-period flexibility curves in Fig. 11(a) are constructed without enforcing the inter-temporal constraints of the BESS. Therefore, the set of flexibility curves presents the maximum available flexibility at each time slot. The curves show that each period has a flexible area that varies depending on network constraints, RES Uncertainty, DER constraints and demand conditions. In Fig. 11(b), the BESS inter-temporal constraints are enforced in the optimization problem. As a result, the available flexibility of time-dependent resources is optimally shared among the hours to maximize the flexibility offered to the upper level.

The comparison of the robust flexibility curves indicates a flexibility reduction throughout the day when considering the inter-temporal constraints. This phenomenon is better shown between 10:00 and 18:00 when the PV generation is high. Additionally, we observe a change on the shape of the curve. An in-depth analysis of the results shows that depending on the search direction, the reactive power requirements and the corresponding losses of the distribution drive a bigger amount of available active power flexibility at different hours.

VI. CONCLUSION

This paper introduces a comprehensive methodology for estimating robust aggregated flexibility at the TSO-DSO interconnection point. The proposed approach leverages scenario-based robust optimization to incorporate the inherent stochasticity of DER and RES, enabling a more accurate and realistic representation of available flexibility, accommodating the variability and uncertainty of power generation and demand. By integrating a joint probability distribution and copulas, the proposed framework accounts for both temporal and spatial correlations among RES time series data within the same region, enhancing the reliability and robustness of the flexibility estimation. Finally, the application of a KDE approach enables the construction of a robust flexibility curve with a specified confidence level, derived from the realizations of available flexibility under various scenarios. The proposed methodology advances the current state of flexibility estimation by addressing the complexities of modern power systems characterized by high penetration of RES. It offers a practical tool for TSOs and DSOs to better coordinate and utilize DERs, ultimately contributing to the stability and efficiency of the power grid.

APPENDIX
JOINT PROBABILITY DISTRIBUTION USING COPULAS CONSIDERING THE SPATIO-TEMPORAL CORRELATION

In modeling spatio-temporal dependence structures, we denote the predicted PV generation for time step t and unit g by

$$P^G_{g,t} \quad , \forall t = 1, 2, \ldots, T, \quad g = 1, 2, \ldots, G \tag{11}$$

Therefore, the total number of random variables that describe the problem under study is equal to $D = T \times G$, and the dependence structure is noted as a D-variate joint probability distribution. The D-variate cumulative distribution function (CDF) is described by

$$F_D(p^G_{1,1}, \ldots, p^G_{T,G}) = Pr(P^G_{1,1} \leq p^G_{1,1}, \ldots, P^G_{T,G} \leq p^G_{T,G}) \tag{12}$$

Based on Sklar's theorem, the independent marginal distributions of the predicted PV generation for each time step and unit can be linked using a copula function, in order to model their dependence structure. The CDF of a copula C is defined as follows

$$\hat{F_D}(p^G_{1,1}, \ldots, p^G_{T,G}) = C(F_{1,1}(p^G_{1,1}), \ldots, F_{T,G}(p^G_{T,G})) \tag{13}$$

where $F_{t,g}$ is the predicted marginal distribution of the g^{th} unit for the t^{th} time step. A copula tinuous random variable is distributed uniformly in $U[0, 1]$. Therefore, to use the copula, the random variables $[P^G_{1,1}, \ldots, P^G_{T,G}]$ must be transformed into a uniform domain through CDF transformation. The CDF transformation can be mathematically written as

$$P^G_{t,g} = F^{-1}_{t,g}(U) \longleftrightarrow U = F_{t,g}(P^G_{t,g}), \ \forall t, g \in [1, T], [1, G] \tag{14}$$

Based on the previous equations, the copula CDF can be represented by

$$C(U_{1,1}, \ldots, U_{T,G}) = \hat{F_D}(F^{-1}_{1,1}(U_{1,1}), F^{-1}_{T,G}(U_{T,G})) \tag{15}$$

According to [30], the Gaussian copula is a good and robust approach for modeling dependency structures for a large number of random variables. The transformed random variables are denoted as $Z_{t,g} = \Phi^{-1}(U_{t,g})$. Second, the joint distribution is modeled using a multivariate Gaussian distribution with mean vector $\boldsymbol{\mu}$ and covariance matrix $\boldsymbol{\Sigma}$. The covariance matrix is obtained from the correlation matrix $\boldsymbol{R}$ by normalizing the variances. The copula density function,

$c_Z(U_{1,1}, \ldots, U_{T,G})$ of the transformed variables can then be expressed as

$$c_Z(z) = \frac{1}{\sqrt{\det(\boldsymbol{\Sigma})}} \exp\left(-\frac{1}{2}(\mathbf{z}-\boldsymbol{\mu})^T \boldsymbol{\Sigma}^{-1}(\mathbf{z}-\boldsymbol{\mu})\right) \quad (16)$$

where z is defined as $[U_{1,1}, \ldots, U_{T,G}]$. Once the Gaussian copula is constructed, it can be used to create realistic scenarios of PV generation, respecting the underlying spatio-temporal correlations.

REFERENCES

[1] I. J. Perez-Arriaga, "The transmission of the future: The impact of distributed energy resources on the network," *IEEE Power Energy Mag.*, vol. 14, no. 4, pp. 41–53, Jul. 2016.

[2] E. Lannoye, D. Flynn, and M. O'Malley, "Evaluation of power system flexibility," *IEEE Trans. Power Syst.*, vol. 27, no. 2, pp. 922–931, May 2012.

[3] J. Ma, V. Silva, R. Belhomme, D. S. Kirschen, and L. F. Ochoa, "Evaluating and planning flexibility in sustainable power systems," *IEEE Trans. Sustain. Energy*, vol. 4, no. 1, pp. 200–209, Jan. 2013.

[4] B. Mohandes, M. S. E. Moursi, N. Hatziargyriou, and S. E. Khatib, "A review of power system flexibility with high penetration of renewables," *IEEE Trans. Power Syst.*, vol. 34, no. 4, pp. 3140–3155, Jul. 2019.

[5] L. N. Ochoa, F. Pilo, A. Keane, P. Cuffe, and G. Pisano, "Embracing an adaptable, flexible posture: Ensuring that future European distribution networks are ready for more active roles," *IEEE Power Energy Mag.*, vol. 14, no. 5, pp. 16–28, Sep. 2016.

[6] M. Z. Liu et al., "Grid and market services from the edge: Using operating envelopes to unlock network-aware bottom-up flexibility," *IEEE Power Energy Mag.*, vol. 19, no. 4, pp. 52–62, Jul. 2021.

[7] M. Heleno, R. Soares, J. Sumaili, R. J. Bessa, L. Seca, and M. A. Matos, "Estimation of the flexibility range in the transmission-distribution boundary," *IEEE Eindhoven PowerTech*, vol. 1, no. 1, pp. 1–20, 2015.

[8] D. Mayorga Gonzalez et al., "Determination of the time-dependent flexibility of active distribution networks to control their TSO-DSO interconnection power flow," in *Proc. Power Syst. Comput. Conf. (PSCC)*, Jun. 2018, pp. 1–8.

[9] S. Riaz and P. Mancarella, "On feasibility and flexibility operating regions of virtual power plants and TSO/DSO interfaces," in *Proc. IEEE Milan PowerTech*, Jun. 2019, pp. 1–6.

[10] P. Cuffe, P. Smith, and A. Keane, "Capability chart for distributed reactive power resources," *IEEE Trans. Power Syst.*, vol. 29, no. 1, pp. 15–22, Jan. 2014.

[11] J. Silva et al., "Estimating the active and reactive power flexibility area at the TSO-DSO interface," *IEEE Trans. Power Syst.*, vol. 33, no. 5, pp. 4741–4750, Sep. 2018.

[12] J. Silva, J. Sumaili, R. J. Bessa, L. Seca, M. Matos, and V. Miranda, "The challenges of estimating the impact of distributed energy resources flexibility on the TSO/DSO boundary node operating points," *Comput. Operations Res.*, vol. 96, pp. 294–304, Aug. 2018.

[13] F. Capitanescu, "TSO–DSO interaction: Active distribution network power chart for TSO ancillary services provision," *Electric Power Syst. Res.*, vol. 163, pp. 226–230, Oct. 2018.

[14] D. A. Contreras and K. Rudion, "Time-based aggregation of flexibility at the TSO-DSO interconnection point," in *Proc. IEEE Power Energy Soc. Gen. Meeting (PESGM)*, Aug. 2019, pp. 1–5.

[15] M. Kalantar-Neyestanaki, F. Sossan, M. Bozorg, and R. Cherkaoui, "Characterizing the reserve provision capability area of active distribution networks: A linear robust optimization method," *IEEE Trans. Smart Grid*, vol. 11, no. 3, pp. 2464–2475, May 2020.

[16] Z. Tan, H. Zhong, Q. Xia, C. Kang, X. S. Wang, and H. Tang, "Estimating the robust P-Q capability of a technical virtual power plant under uncertainties," *IEEE Trans. Power Syst.*, vol. 35, no. 6, pp. 4285–4296, Nov. 2020.

[17] N. Savvopoulos and N. Hatziargyriou, "Estimating operational flexibility from active distribution grids," in *Proc. 17th Int. Conf. Eur. Energy Market (EEM)*, Sep. 2020, pp. 1–6.

[18] S. Riaz and P. Mancarella, "Modelling and characterisation of flexibility from distributed energy resources," *IEEE Trans. Power Syst.*, vol. 37, no. 1, pp. 38–50, Jan. 2022.

[19] M. Jafarian, A. Nouri, V. Rigoni, and A. Keane, "Real-time estimation of support provision capability for poor-observable distribution networks," *IEEE Trans. Power Syst.*, vol. 38, no. 2, pp. 1806–1819, Mar. 2023.

[20] G. K. Papazoglou, A. A. Forouli, E. A. Bakirtzis, P. N. Biskas, and A. G. Bakirtzis, "Estimating the feasible operating region of active distribution networks using the genetic algorithm," in *Proc. IEEE PES GTD Int. Conf. Expo.*, May 2023, pp. 1–11.

[21] F. Klein-Helmkamp, T. Offergeld, and A. Ulbig, "Cluster-based analysis of feasible operating regions for aggregated energy storage systems," in *Proc. IEEE Belgrade PowerTech*, Jun. 2023, pp. 1–12.

[22] K. Girigoudar and L. A. Roald, "Identifying secure operating ranges for DER control using bilevel optimization," *IEEE Trans. Smart Grid*, vol. 15, no. 3, pp. 2921–2933, May 2024.

[23] D. Yan, S. Huang, and Y. Chen, "Real-time feedback based online aggregate EV power flexibility characterization," *IEEE Trans. Sustain. Energy*, vol. 15, no. 1, pp. 658–673, Jan. 2024.

[24] M. Zhang, Y. Xu, X. Shi, and Q. Guo, "A fast polytope-based approach for aggregating large-scale electric vehicles in the joint market under uncertainty," *IEEE Trans. Smart Grid*, vol. 15, no. 1, pp. 1–18, Jul. 2023.

[25] G. Papazoglou and P. Biskas, "Review of methodologies for the assessment of feasible operating regions at the TSO–DSO interface," *Energies*, vol. 15, no. 14, p. 5147, Jul. 2022.

[26] N. Savvopoulos, C. Y. Evrenosoglu, T. Konstantinou, T. Demiray, and N. Hatziargyriou, "Contribution of residential PV and BESS to the operational flexibility at the TSO-DSO interface," in *Proc. Int. Conf. Smart Energy Syst. Technol. (SEST)*, Sep. 2021, pp. 1–6.

[27] J. Lofberg, "YALMIP: A toolbox for modeling and optimization in MATLAB," in *Proc. IEEE Int. Conf. Robot. Autom.*, Sep. 2004, pp. 1–29.

[28] A. Wächter and L. T. Biegler, "On the implementation of an interior-point filter line-search algorithm for large-scale nonlinear programming," *Math. Program.*, vol. 106, no. 1, pp. 25–57, Mar. 2006.

[29] T. Konstantinou and N. Hatziargyriou, "Day-ahead parametric probabilistic forecasting of wind and solar power generation using bounded probability distributions and hybrid neural networks," *IEEE Trans. Sustain. Energy*, vol. 14, no. 4, pp. 2109–2120, Oct. 2023.

[30] F. Golestaneh, H. B. Gooi, and P. Pinson, "Generation and evaluation of space–time trajectories of photovoltaic power," *Appl. Energy*, vol. 176, pp. 80–91, Aug. 2016.

NIKOLAOS SAVVOPOULOS (Member, IEEE) received the Diploma degree in electrical and computer engineering from the Democritus University of Thrace, Greece, in 2014, and the M.Sc. degree in electrical power engineering from RWTH Aachen University, Germany, in 2018. He is currently pursuing the Ph.D. degree with the School of Electrical and Computer Engineering, National Technical University of Athens, Greece. From 2016 to 2018, he was with the Power and Energy Systems Group, Automation Department, ABB Corporate Research Center, Baden–Dättwil, Switzerland. His research interests include the optimization of power system operation, flexibility provision from distributed energy resources, and TSO-DSO coordination.

NIKOS HATZIARGYRIOU (Life Fellow, IEEE) is currently a Professor Emeritus of power systems with the National Technical University of Athens. He has over ten years of industrial experience, having served as the Chairman and the CEO of Hellenic Distribution Network Operator (HEDNO), and the Executive Vice-Chair and the Deputy CEO of Public Power Corporation (PPC), responsible for the transmission and distribution divisions. He chaired the EU Technology and Innovation Platform on Smart Networks for Energy Transition (ETIP-SNET). He is the author of the book ''*Microgrids: Architectures and Control*.'' He has participated in more than 60 research and development projects funded by EU Commission, electric utilities, and industry, encompassing both fundamental research and practical applications. He has been listed in the Thomson Reuters lists of the top 1% most cited researchers in 2016, 2017, and 2019. He was a recipient of several prestigious awards, including the 2017 IEEE/PES Prabha S. Kundur Power System Dynamics and Control Award, the 2020 Globe Energy Prize, and the 2023 IEEE/PES Herman Halperin Electric Transmission and Distribution Award. He is an Honorary Member of CIGRE and serves as the Editor-in-Chief at Large for IEEE PES journals.

HANNU LAAKSONEN (Member, IEEE) received the M.Sc. (Tech.) degree in electrical power engineering from Tampere University of Technology, Tampere, Finland, in 2004, and the Ph.D. (Tech.) degree in electrical engineering from the University of Vaasa, Vaasa, Finland, in 2011. His employment experience includes working as a Research Scientist with VTT Technical Research Centre of Finland and the University of Vaasa. He has previously worked as the Principal Engineer of ABB Ltd., Vaasa. He is currently a Professor of electrical engineering with the University of Vaasa. He is also the Research Team Leader and the Manager of the Smart Energy Master's Program, School of Technology and Innovations, Flexible Energy Resources, University of Vaasa. His research interests include the control and protection of low-inertia power systems and microgrids, active management of distributed and flexible energy resources in future smart energy systems, and future-proof technology and market concepts for smart grids.